

# International Conference on Space Optics—ICSO 2012

Ajaccio, Corse

9–12 October 2012

*Edited by Bruno Cugny, Errico Armandillo, and Nikos Karafolas*



## *Development of high precision and cryogenic lens holders*

*A. Reutlinger*

*Anton Boesz*

*A. Mottaghibonab*

*P. Eckert*

*et al.*



## Development of High Precision and Cryogenic Lens holders

C.Gal\*<sup>a</sup>, A. Reutlinger<sup>a</sup>, A. Boesz<sup>a</sup>, T. Leberle<sup>a</sup>, A. Mottaghibonab<sup>a</sup>, P. Eckert<sup>a</sup>, M. Dubowy<sup>a</sup>,  
H.Gebler<sup>a</sup>, F. Grupp<sup>bc</sup>, N. Geis<sup>b</sup>, A. Bode<sup>b</sup>; R. Katterloher<sup>b</sup>, R. Bender<sup>bc</sup>

<sup>a</sup>Kayser-Threde GmbH, 48. Wolfratshauer Str., Munich, Germany, D-81379

<sup>b</sup>Max-Planck-Institut für extraterrestrische Physik, Giessenbachstr., Garching, Germany, D-85748

<sup>c</sup>Universitäts Sternwarte München, Scheinerstr 1, Munich, Germany, D-81679

### ABSTRACT

The optical system of the Near Infrared Spectrometer and Photometer (NISP) of the EUCLID mission consists mainly of a filter and grism wheel and 4 aspherical lenses with large diameters up to 170 mm. The single lenses require a high precision positioning at the operational temperature of 150 K. An additional design driver represents the CaF<sub>2</sub> material of a lens, which is very sensitive wrt brittleness.

The technical maturity of the combination of single features such as CaF<sub>2</sub>, large diameter (and mass), high precision and cryogenic conditions is considered as low. Therefore, a dedicated pre-development program has been launched to design and develop a first prototype of lens holder and to demonstrate the functional performance at representative operational conditions.

The 4 lenses are divided into 3x lenses for the Camera Lens Assembly (CaLA) and 1x lens for the Corrector Lens Assembly (CoLA). Each lens is glue mounted onto solid state springs, part of an adaption ring. The adaption ring shall provide protection against vibration loads, high accuracy positioning, as well as quasi load free mounting of the lens under operational conditions. To reduce thermomechanical loads on the lens, the CTE of the adaption ring is adapted to that of the lens. The glue between lens and solid state spring has to withstand high tension loads during vibration. At the operational temperature the deviating CTE between glue and lens/adaption ring introduces shear loads into the glue interface, which are critical, in particular for the fragile CaF<sub>2</sub> lens material. For the case of NISP the shear loads are controlled with the glue pad diameter and the glue thickness.

In the context of the development activity many technology aspects such as various solid state spring designs, glue selection and glue handling have been investigated. A parametric structural model was developed to derive the specific design feature of each ring, such as spring force, number of springs, eigenfrequency, etc.

This paper presents the design of the adaption ring in conjunction with test results from functional verification. These results are presented on behalf of the EUCLID consortium.

**Keywords:** EUCLID, cryogenic, spectrometer, photometer, high precision, interferometer, fiber based distance sensor, verification

## 1 INTRODUCTION

### 1.1 Science Backgrounds of EUCLID

The Near-Infrared Spectrometer and Photometer (NISP) is one of the key instruments on-board the Euclid mission. The instrument is located in the payload of the Euclid satellite, and it is initially planned to be operated at 150 K, except the detectors that are cooled to about 100 K. The operating wavelength range of the instrument is 1.0  $\mu\text{m}$  – 2.0  $\mu\text{m}$ . The Euclid mission is optimized for two primary cosmological probes: Weak Lensing (WL) and Baryonic Acoustic Oscillations (BAO) [1]. The two operating modes of the NISP instrument, the photometry and the spectroscopy mode, are designed for the WL and BAO probes respectively. The photometry mode of the NISP instrument is a crucial part of the weak lensing science probe. This mode will be used to supplement the visible shape measurements with multiband, near-infrared photometry of all the imaged galaxies. This data will be used for photometric estimations of galaxy redshifts. With the large survey area ( $>20,000 \text{ deg}^2$ ) and its multiple near-infrared bands, the photometry mode of the NISP instrument will also yield a highly valuable dataset for legacy science.

BAOs are wiggle patterns imprinted in the clustering of galaxies which provide a standard ruler to measure dark energy and the expansion in the universe. BAO requires a high near-infrared spectroscopic capability to measure accurately galaxies redshifts at  $z > 1$  and the ability to survey the entire extra-galactic sky. This kind of surveys will also allow measurements of galaxy clusters and redshift space distortions that will provide additional measurements of the cosmic geometry and structure growth.

\*csaba.gal@kayser-threde.com; phone +49-89-724-95-195; fax +49-89-724-95-291; <http://kayser-threde.com>

A central design driver for Euclid is the ability to provide tight control of systematic effects in space-based conditions. Together, these information will be able to constraint the dark energy parameters and test accurately the cosmological model. The spectroscopic redshift survey will give census of more than  $10^8$  H-alpha emission line galaxies over most of the sky in the redshift range of  $z = 0.5..2$ .

## 1.2 NISP Instrument

The objective of the study phase is to establish the technical definition the NISP Instrument at system level and the high precision lens holder design at sub-system level that complies with its technical requirements specification. The success of the program has major impact on the advancements of the EUCLID project, as well as, technological development achievements are meaningful for future programs employing large lens mounts with high positioning accuracy.

Figure 1-1 illustrates the NISP instrument, which consists of the optical bench, the detection system (16 H2RG detectors), filter and grism wheel mechanisms as well as the optical system, which is subdivided into the Corrector Lens Assembly (CoLA) and the Cameral Lens Assembly (CaLA).

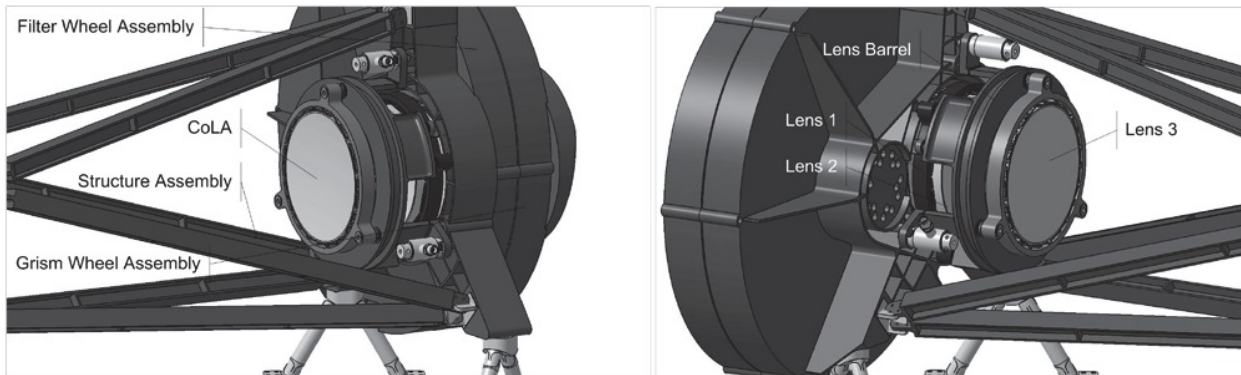


Figure 1-1 NISP instrument design

The CaLA accommodates three aspherical lenses (L1: CaF<sub>2</sub>; L2 & L3: LF5G15), which are mounted by using adaption rings inside a lens barrel as illustrated in Figure 1-2.

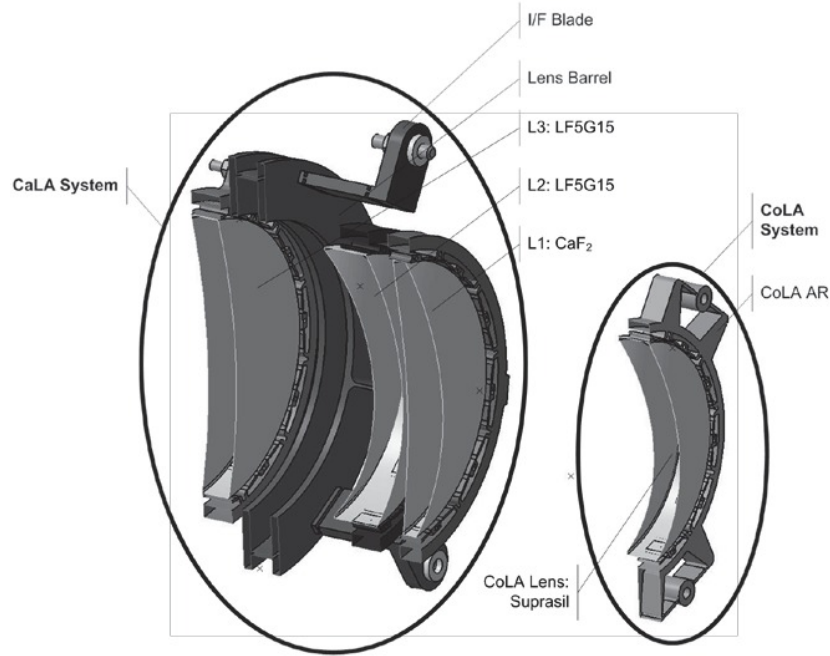


Figure 1-2 CoLA and CaLA designs

The accommodation of the lenses with the required position accuracy and operation temperature has been assessed as critical due to the positioning requirement, the large dimension of up to 170 mm and the cryogenic conditions. The required Technology Readiness Level (TRL) is <5 and is therefore critical with respect to mission selection and implementation. In the context of the EUCLID Pre-Development project, carried out by KT, a representative lens holder has been developed and successfully tested. The requirements and test results are reported in the following.

### 1.3 Adaption Ring Design

Each lens is mounted in an adaption ring (AR). During the analytical activities several concepts have been investigated considering material selection, manufacturing processes, operating conditions, etc. and selected down for candidate concept and verification tests. Also the production, assembly, integration and test operations and maintenance of the lens holder are the technical baselines for the concept. The results of the analytical calculations led to the AR design illustrated in Figure 1-3, where the AR of the CaF<sub>2</sub> lens is presented as an example. The lens is supported by complex spring flexures that are attached to the lens by applying space qualified epoxy bond [2]. The bonding pad diameter for each spring shall have the same dimension and thickness, otherwise, asymmetric deformation of the lens is introduced, and hence, the accurate position is not guaranteed. The AR material has similar CTE as the lens material to avoid significant stress in the lens material. Also the interface to the lens barrel is realized by means of flexure blades that allow both the high position accuracy of lens mounting and the low lens deformation introduced by CTE mismatch of the support structure.



Figure 1-3 Adaption Ring design

This design concept allows a soft lens mount over the required wide temperature range and provides sufficient mechanical strength to survive the launch loads.

## 2 REQUIREMENTS AND DESIGN DRIVERS

The optical system optimization resulted in the following 3 material types of the NISP lenses: fused silica, CaF<sub>2</sub>, and LF5G15. One of the most important functional requirements of the AR is the low stress support of the lens at the operation temperature of 150 K. In case of CaF<sub>2</sub> the effect is the most critical, since it is birefringent. The AR shall be designed to withstand the heavy vibration loads during launch and also adequately protect the lens. As an example, Table 1 shows the applied random vibration loads for the CaF<sub>2</sub> lens.

Table 1 Random test specification

Frequency (Hz)	Level (0-peak)	Sweep rate
5-21	11 g	4 Oct/min
21-60	20g	i.e.
60-100	6g	

The AR has to perform all required operations in any spatial orientation with and without presence of gravity. Lens fabrication errors and mounting corrections shall be compensated by alignment of each AR individually with respect to well defined reference points of the system. For this adjustment procedure the required position precision of the lens (s. Table 2) are attained by using polished shims underneath the interface of the AR. Also the glue used for lens fixing to the AR shall be adequate for cryogenic temperatures and shall survive the vibration loads at ambient conditions. Furthermore, the glue shall withstand the tensile- and shear stresses at cryogenic conditions.

To determine the manufacturing and alignment accuracies of the lens a detailed tolerancing analysis has been performed. Usual mechanical tolerance types are considered for each lens surface and lens as elements. Additionally, transmitted WFE has been taken into account to assess real operation conditions. Each lens has an aspherical surface, where very high accuracy is required. To overcome the technical difficulties during aspherical lens polishing sequential manufacturing procedure has been considered. This means that the intrinsic WFE of the first three aspherical lenses are compensated by the last one. Only this technological way provides the necessary imaging quality of the optical system. After the alignment procedure of the instrument has been completed the alignment shall be stable on ground during system integration and also during flight to achieve the required optical performance. Typical position tolerance of alignment and manufacturing is presented in Table 2.

Table 2 Alignment accuracy and position stability requirements of the lens

	Axial [ $\mu\text{m}$ ]	Radial [ $\mu\text{m}$ ]	Tilt [arcsec]
Assembly	$\pm 15$	$\pm 10$	$\pm 10$
Stability	$\pm 2$	$\pm 3$	$\pm 2$

The operating temperature is assumed to be stable within a 0.3°K range, which is maintained by applying an active thermal control of the unit.

The small position and angular tolerance requirements drive the required accuracy of the metrology system, which is defined to be <1µm.

### 3 TEST OVERVIEW

The AR's tested during the test campaign undergo the test sequence as illustrated in Figure 3-1. In the following chapters a short description of each test is given.

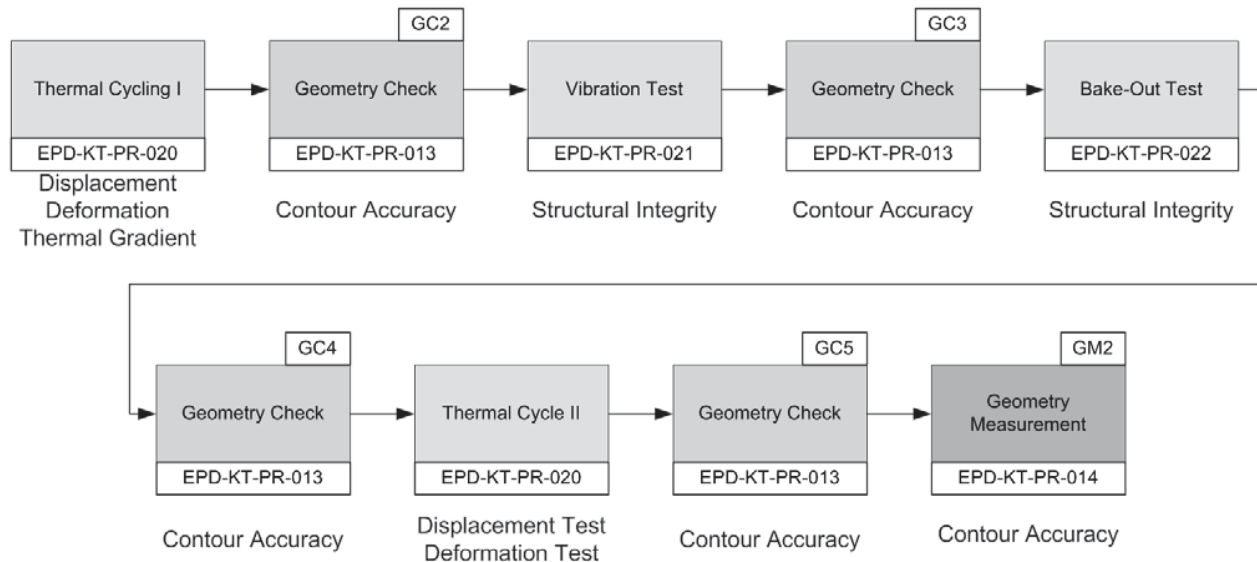


Figure 3-1 AR test sequence

#### 3.1 Thermal Cycling I + II

The AR assembly undergoes a thermal test, where the environment temperature of the AR is changed between RT (300 K) and operation temperature of 150 K (OPS). The test environment is accomplished by means of a cryostat system that cools down and heats up the test equipment to required temperature plateaus, as seen in Figure 3-2. The very first thermal cycle is dedicated to reduce settling effects in the measurement test setup. In the first thermal cycle sequence (RT1 – OPS1 – OPS2 – OPS3 – RT2) the lens position and rotation (tip, tilt) relative to the AR is detected by distance measurement sensors and the specified accuracy and repeatability is assessed. Moreover, the lens surface deformation is assessed at different temperatures with interferometric measurements and the transmitted WFE distortion is determined. For further optical analysis and performance verification the achieved temperature gradient over the lens surface is evaluated applying several temperature sensors.

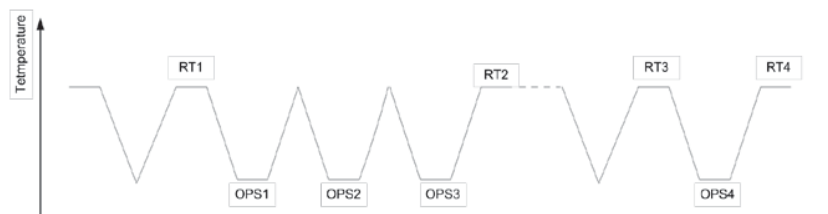


Figure 3-2 Thermal cycles applied for each AR

Between RT2 and RT3 further environmental tests (vibration, bake-out) are performed with the AR assembly. The second thermal cycle sequence (RT3 – OPS4 – RT4) verifies the reproducibility of the first thermal cycle of RT1 to RT2 and verifies the stability performance of the AR design with respect to vibration loads.

### 3.2 Geometry Check

To detect any displacement of the lens relative to the AR, geometry check has been performed after each thermal cycling. The geometry measurement detects damages or deformations of the AR after each cycle. The inductive distance sensors are able to measure relative and absolute distance changes with accuracy of the order of  $0.1 \mu\text{m}$ . 12 x TESA GT21 sensors are mounted in radial and axial directions and the difference of distance is determined. The measured axial values are used to calculate the angular changes (tip / tilt) of the lens. Figure 3-3 illustrates the arrangement of the sensors (2 x 3) to measure the relative displacement between the lens and AR in radial direction.

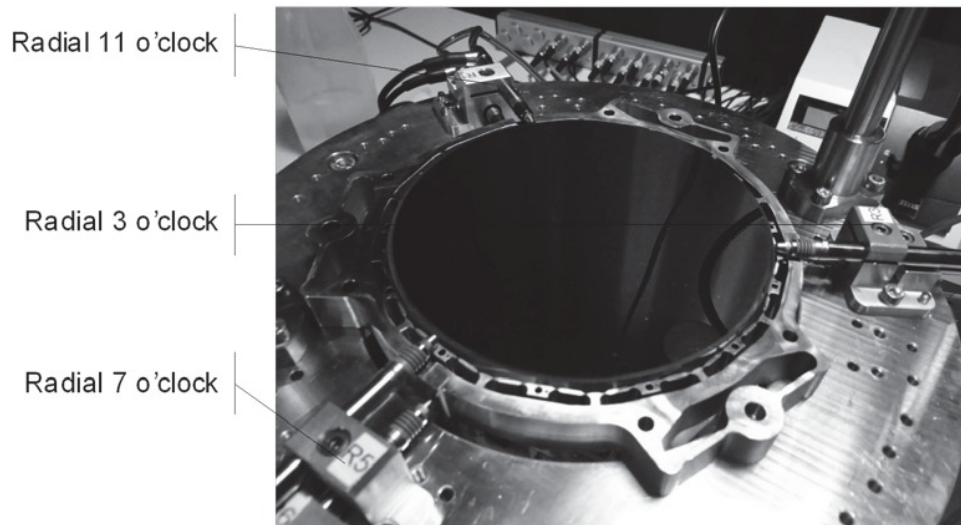


Figure 3-3 Geometry check measurement of the AR assembly

4 geometry checks were performed of each AR's after thermal-, vibration-, and bake out tests in order to detect any setting effects, damages or deformations. Finally, the position changes are transferred into translation and rotation values of the lens ( $T_x$ ,  $T_y$ ,  $T_z$ ,  $R_x$ ,  $R_y$ ) and the data are compared with the values assessed by the optical tolerancing.

### 3.3 Vibration Test

Vibration tests have been carried out during the test campaign to verify the structural integrity of the AR assemblies:

- Resonance search (low load sine vibration prior to full load tests)
- Sine vibration
- Resonance search (low load sine vibration after full load sine vibration)
- Low level random vibration
- Broad band random vibration
- Resonance search (low load sine vibration after full load random vibration)

During the vibration test the AR is mounted to a 30 mm thick adapter plate made of Aluminum. This plate is fastened again on an Aluminum cube to perform the test in the three mutually perpendicular test axes, as seen in Figure 3-4.

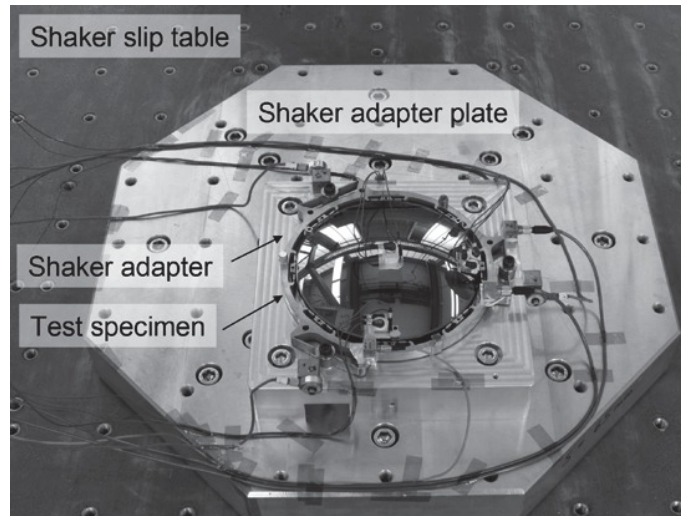


Figure 3-4 AR assembly mounted on the shaker adapter

The accelerometers measure the vibration of the AR and lens at the defined positions according to specified points and the measure data are recorded.

### 3.4 Bake-Out Test

The lens is mounted to the AR by means of space qualified adhesive. The curing procedure of the used glue of DP490 takes place at room temperature; however, degassing has to be performed at 50 °C temperature. The typical temperature curve as a function of time is presented in Figure 3-5.

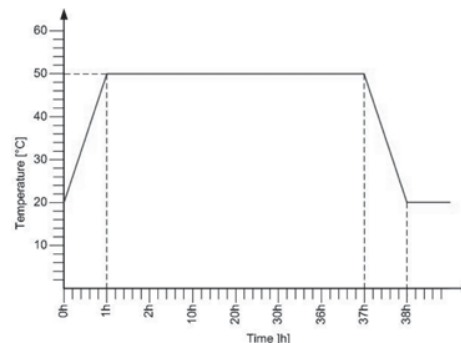


Figure 3-5 Bake-out temperature curve

During the test several temperature sensors are mounted to the AR as well as on the lens to monitor the temperature distribution on the test sample. For the AR assembly the bake-out test represents an additional thermal load, therefore, the geometry and relative lens position to the AR is measured before and after the test, as described in 3.2.

### 3.5 Geometry Measurement

The verification of the AR after manufacturing was performed with geometrical measurements. Via a coordinate measurement machine of type Zeiss PRISMO 7, the contour accuracy of the AR was measured to verify the defined manufacturing tolerances and determination of important values such as inner diameter of the AR, planarity and parallelism of reference planes and measurement planes used during the gluing process.

Any non-reversible change in the AR material during thermal cycling or plastic deformation effects in the adhesive might result in displacement and/or deformation of the lens, therefore the geometry measurement is of crucial importance. In the context of the AR test campaign the first geometry measurement was performed after the AR assembly and was repeated at the end of the AR test campaign to determine and compare non-reversible deformations of the AR and lens in representative environments.

## 4 METROLOGY SYSTEM

### 4.1 Fiber Optic Distance Sensors

To reach the main objective of the AR verification program the relative spatial movement between AR and lens is measured with Philtec fiber sensors [3] during the cooling down process inside the cryostat. This displacement measurement verifies the position tolerances and stability of the lenses at the operating temperature.

The operating principle of the fiber sensor bases on two fiber bundles, which are arranged side-by-side. The emitted light exits one bundle is then reflected from the target and returns to the sensor. A radiometric calculation of the incident and reflected signals provides the distance measurement. Philtec sensors measure contact free, which is of crucial importance for sensitive space qualified hardware. Further benefit of the system is the small sensor head with the even smaller target spot size that allows access to hard reachable targets. Figure 4-1 illustrates the selected displacement sensor and the arrangement with the test object.



Figure 4-1 Fiber optic Displacement sensor from Philtec (left) and their installation to the measurement setup (right)

#### 4.1.1 Calibration of Fiber Optic Distance Sensors

The aim of Distance Sensor Calibration is to characterize and quantify the behavior of the Philtec sensors at cryogenic conditions and to determine the movement of the Sensor Mount itself, which is then subtracted from the complete distance change between the lens and the adaption ring.

Following calibration procedures have been conducted for the displacement measurement:

- Target characterization,
- Linearity calibration,
- Sensor characterization,
- Sensor Mount characterization.

Two types of sensors are used, RC60 for radial measurements with a measurement range from 0 to 3 mm and RC100 with a measurement range from 0 to 5 mm. All displacement sensors are mounted inside the sensor mount and measure the lens and the AR in axial and radial directions. The sensor mount consists of a quasi-zero CTE material ( $\sim 0,2 \times 10^{-7}$  m/m\*K). Due to the low CTE the shrinkage effects of the SM can be neglect and used as a reference to measure shrinkage effects of AR, lens and reference structure. Figure 4-2 represents test setup inside the cryostat.

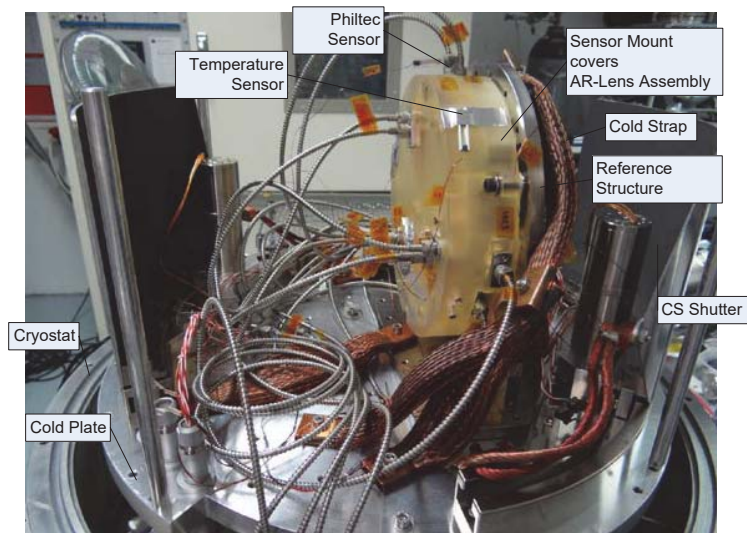
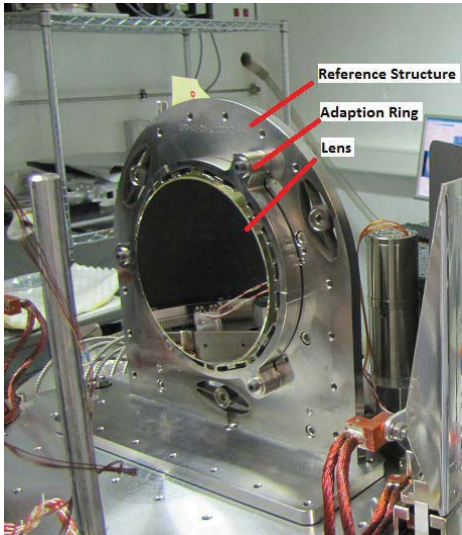


Figure 4-2 Test setup: Opened Cryostat without Sensor Mount (left), Sensor Mounted with axial and radial positioned Philtec sensors (right)

**Target Characterization**

The measurement principle of the Philtec sensor is highly dependent on the surface of the measured object like roughness, flatness and reflectivity. High reflectivity improves the measurement performance.

The distance measurement of the AR assembly has to be performed on three different surfaces: lens surface (coated and uncoated), lens edge (uncoated), and grinded reference areas on the AR. Further impact of the measurement on the determined distance is the different lens and AR materials. In order to improve the measurement performance mirrored discs have been applied on the AR reference areas to improve and harmonize the surface reflectivity.

**Linearity calibration**

The objective of linearity calibration is the absolute calibration of each sensor. They shall be calibrated for later measurement targets (related calibration). A high precision linear stage travels the sensor in front of the target in defined step and the sensor output and the stage position are recorded. A typical calibration curve is shown in Figure 4-3.

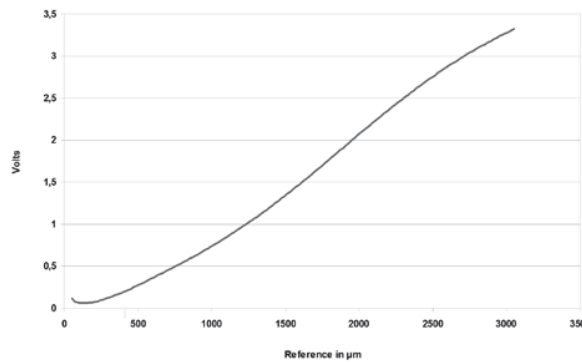


Figure 4-3 Calibration curve at room temperature

**Sensor characterization**

The calibration curve measured at 300K is not applicable for measurements performed at 150K. Furthermore, each sensor has individual behaviour due to its slightly different sensor head, which is a material composite of glass fiber, epoxy glue and metallic housing. Hence, each sensor has been characterized individually at low cryogenic temperatures. For the test a dedicated sensor calibration tool has been prepared, which is also made of a quasi-zero CTE ceramic

material and hence the equipment shrinkage does not impact the shrinkage of the sensor assembly. The design of test setup in cross section is illustrated in Figure 4-4.

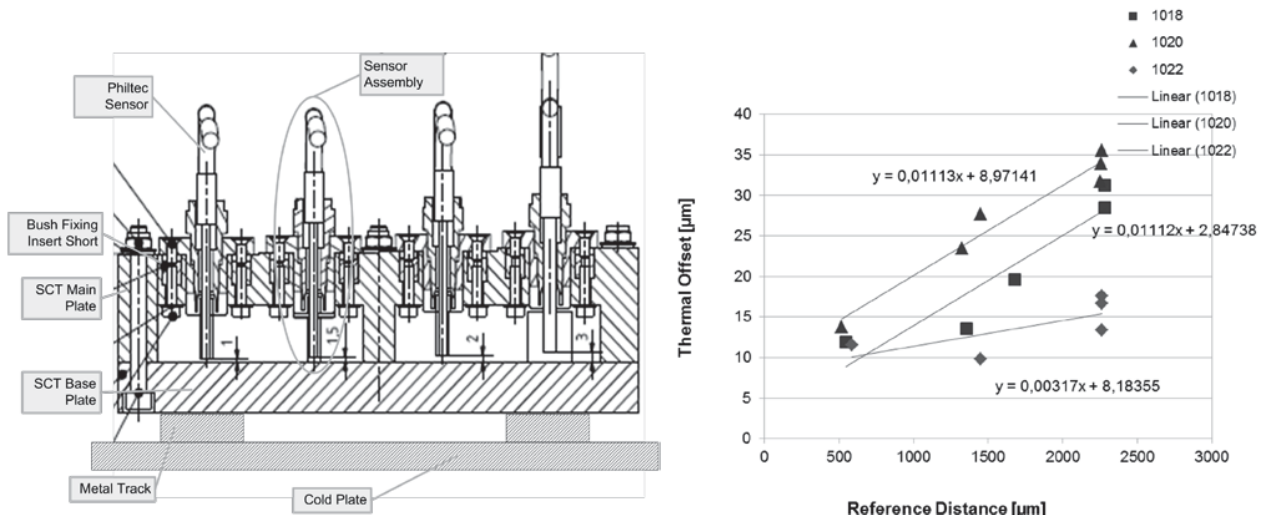
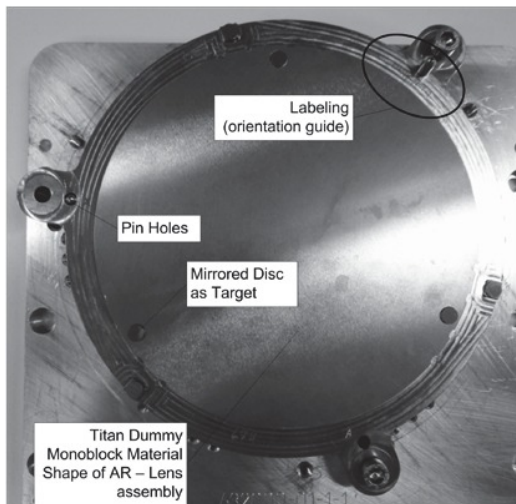


Figure 4-4 Test setup of the sensor calibration tool (left) and sensor characterization diagram (right)

The sensors are mounted by their sensor fixing bushes (Invar) and the distances to the base plate are adjusted to have different sensor offsets (1-3 mm in 0.5 and 1 mm steps respectively). The measured distances of each sensor are plotted as a function of sensor shrinkage. A typical calibration curve in Figure 4-4 represents a trend line of sensor, which is used as correction function for all later thermal cycle measurements.

#### Sensor Mount Characterization

The calibration procedure characterizes the impact of the sensor mount and sensor fixing on the distance measurement if the test equipment is cooled down to 150 K. For the setup a full Titanium design is constructed including the reference structure, the AR assembly and used as test object. The material parameters for Titanium are well known and hence the shrinkage of the assembly can be precisely calculated, if the temperature of the unit is also measured. From the measured and calculated data the distance change can be determined, which represents the effect of the sensor mount itself.



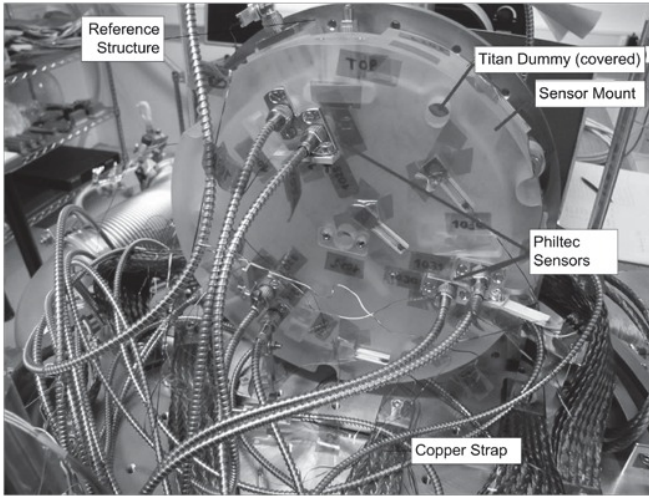


Figure 4-5 Titan Dummy (left) and test setup of Titan Dummy test (right)

## 4.2 Interferometer

In the course of thermal cycling the lens surface deformation is measured directly with interferometric measurements using MiniFiz 100 interferometer [4]. The interferometer allows high precision (10-20 nm) measurements of lens surface deformations caused by mechanical-, thermal-, thermal gradient-, and gravity loads. Figure 4-6 illustrates the interferometer measurement setup with the cryostat opened.

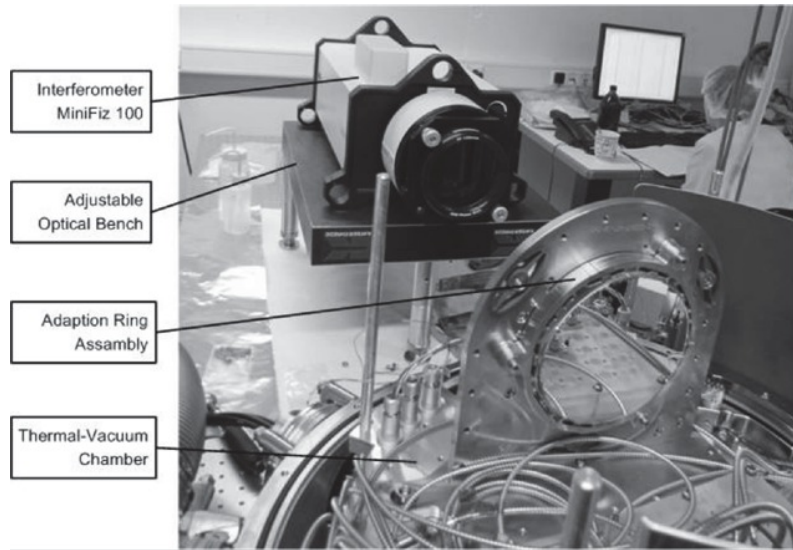


Figure 4-6 Interferometer test setup with adjustable optical bench

The lens deformation assessment approach is based on sequential measurements of the AR assembly. With this measurement procedure it is possible to draw conclusions with regard to the impacts of the different assembly steps, vibration loads, and operation temperature changes (RT to 150 K).

## 5 TEST RESULTS

During the test campaign 3 different AR-lens material combinations have been tested successfully, however due to the brittleness of the  $\text{CaF}_2$  lens material the corresponding AR assembly is considered as the most critical one. For this reason, the  $\text{CaF}_2$  AR assembly is presented here more in detail and the results of the other AR's are only denoted. The image of the integrated  $\text{CaF}_2$  lens is illustrated in Figure 5-1.



Figure 5-1 Assembled AR with the CaF<sub>2</sub> spherical dummy lens

### 5.1 Results of Thermal Cycling I + II

The AR system CaF<sub>2</sub> spherical has performed excellent, since the translation and the rotation values of the lens relative to the AR is well within the requirement, as presented in Table 3.

Table 3 Displacement results of the lens after thermal cycle I and II

Lens to AR	Tx	Ty	Tz	Rx	Ry
Requirement	±10 µm	±10 µm	±15 µm	±10 arcsec	±10 arcsec
Thermal Cycle I	10,02 µm	-0,77 µm	10,57 µm	-19,2 arcsec	-3,01 arcsec
Thermal Cycle II	11,75 µm	0,18 µm	11,59 µm	-15,93 arcsec	-1,14 arcsec

The radial sensors measured the translation of the lens relative to the AR during thermal cycle I and II at RT and OPS temperatures. The values are also graphically presented in Figure 5-2 left, where the direction of motion is well seen at the indicated two temperatures. In Figure 5-2 right the rotation of the lens in x and y directions (tip, tilt) relative to the AR can be observed at the different temperatures.

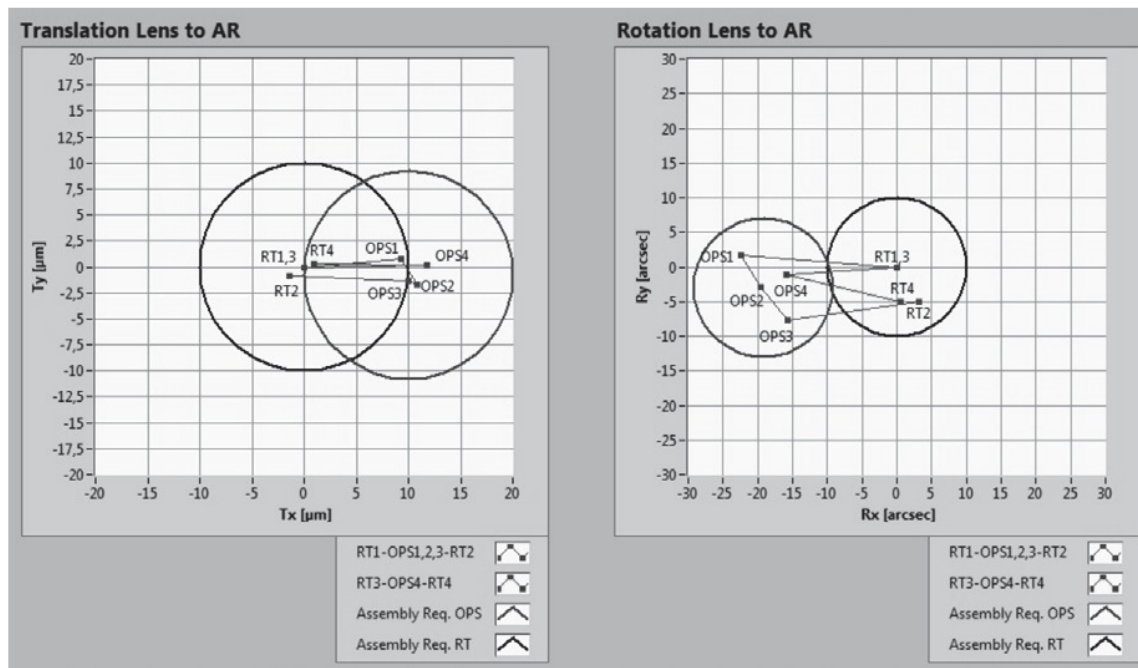


Figure 5-2 AR CaF<sub>2</sub> Spherical: Repeat accuracy of translation (left), repeat accuracy of rotation (right). The circles reveal the tolerance requirements of  $\pm 10 \mu\text{m}$  and  $\pm 10 \text{arcsec}$ , respectively.

## 5.2 Deformation Test Results

The deformation characterization of the AR assembly is evaluated from difference of two interferometric measurements performed at RT and at 150 K temperatures. The result of the evaluation shows slight astigmatic deformation of the lens surface, which corresponds to about 2.7 nm RMS transmitted wavefront error per lens surface or 3.8 nm per lens. This value is well within the requirement of 32 nm and the design reveals the low stress mounting of the lens at the relevant temperature range. The deformation of the front and rear surface of the glass is strongly correlated, therefore the real wavefront deformation is even smaller.

## 5.3 Geometry Check Results

5 geometry checks have been performed for the AR assembly during the test campaign to detect settling effects or damages after the thermal cycles, vibration tests and the bake-out test. The high precision sensors measured small changes of the lens position that are in the order of  $< 1 \mu\text{m}$  for translations and  $< 4 \text{arcsec}$  for rotation that are well within the requirements.

## 5.4 Vibration Test Results

The vibration test has been successfully completed. The specified test levels have been achieved for all tests and the AR assembly withstood all vibration loads without any damage. The resonance search before and after the tests doesn't show any differences in natural frequencies. The first natural frequency is measured to be 323.4 Hz that fits very well to the analytically calculated value of 324 Hz. The sine tests of the AR reveal rigid body motion of the specimen if test frequency range is between 5 Hz and 100 Hz, which shows the adequate design of the ring.

The random tests are performed in x, y, and z directions, however here only the x direction is presented. In x direction a nominal level of 20.3 g RMS is performed with a notched random profile, as illustrated in Figure 5-3. The resulting input g RMS is 13.7. The input and response spectrum is depicted in Figure 5-3 right. The maximum load level during the random vibration test with notching was 60.5 g RMS in x-direction, which is slightly above the design limit load of 60 g RMS.

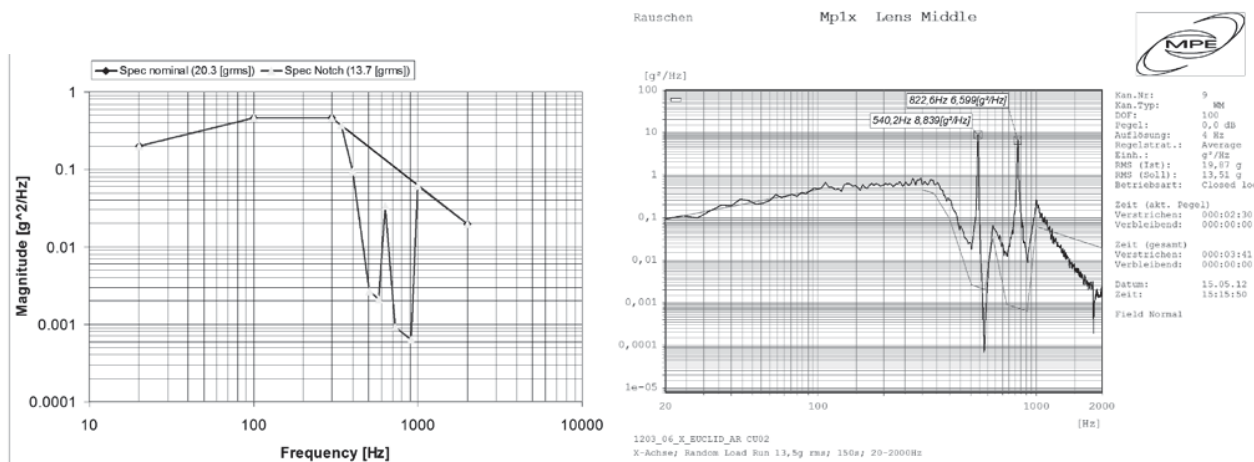


Figure 5-3 Nominal and notched spectrum for x axis high level (0dB) random test (left), Input spectrum and response spectrum for vibration test in x-direction (right)

### 5.5 Bake-out Test Results

The AR assembly with the CaF<sub>2</sub> lens has withstood the bake-out test. Any macro cracks on the lens surface and lens edge (glue pads) after visual with a green laser have not been detected. Comparison of geometry check results does not show any deformation, displacement or settling effect after bake-out.

### 5.6 Geometry Measurement Results

Geometrical measurements have been performed after manufacturing and assembly by means of measurement points that characterize the geometry of the AR assembly. The test results show that the form deviation remains <1 μm in all cases, which is fully compliant with the requirements.

## 6 CONCLUSION

The verification campaign of the AR assembly including the CaF<sub>2</sub> lens has been successfully accomplished at KT, the following milestones have been performed

- Calibration of metrology system for operation under cryogenic condition,
- Design of AR that provides the high mechanical and thermal stability for the the lens,
- Successful qualification test that prove the required TRL >5.of the AR assembly.

## 7 ACKNOWLEDGEMENTS

The development of the adaption rings was performed under a contract from MPE, Garching. The MPE EUCLID participation is supported by DLR grant 50 OO 1101. The authors would like to acknowledge Max-Planck-Institute for Extraterrestrial Physics (Garching), Asphericon (Jena) and the Institute for Lightweight Structure (LLB), Technical University Munich for its co-operation.

## REFERENCES

- [1] R. Laureijs et al, "Euclid Mapping the geometry of the dark Universe", Definition Study Report, ESA/SRE(2011), Version 1.0, (2011)
- [2] A. Reutlinger, et al., "Glue Test Results for High-Precision Large Cryogenic Lens Holder", Proc. SPIE 8450-74, (2012).
- [3] <http://www.philtec.com>
- [4] <http://www.diffraction.com>